2007 IEEE International Conference on
Robotics and Automation
Roma, Italy, 10-14 April 2007

Design of an Autonomous Jumping Microrobot

Sarah Bergbreiter and Kristofer S. J. Pister
Berkeley Sensor and Actuator Center
497 Cory Hall
Berkeley, CA 94720, USA
{sbergbre, pister}@eecs.berkeley.edu

Abstract – **This paper presents the design and initial results for an autonomous jumping microrobot. At the millimeter size scale, jumping can offer numerous advantages for efficient locomotion, including dealing with obstacles and potentially even latching onto other larger mobile hosts. Robot design is divided into four primary areas: energy storage, actuation, power, and control. Like its biological inspiration, the flea, a jumping microrobot requires an energy storage system to store energy and release it quickly to jump. Silicone micro rubber bands have been fabricated and assembled into the microrobot for this task. To stretch these micro rubber bands, electrostatic inchworm motors are chosen as actuators due to their high forces, long throw, and low input power requirements. Finally, solar cells and a microcontroller have been chosen to power and control the microrobot. A small-scale version of this system has been prototyped with the solar cells and a simple 4-bit microcontroller driving an inchworm motor. Separately, an inchworm motor has been demonstrated pulling and storing 4.9 nJ of energy in a micro rubber band. Finally, initial tests with a probe-loaded robot prototype have demonstrated a microrobot which can potentially jump 1.2 cm straight up.**

Index Terms *– Micro/Nano Robots, Jumping Robots, Biologically-Inspired Robots.*

I. Introduction

Mobile autonomous microrobots, defined as millimeter-sized mobile robots with power and control on board, offer numerous advantages due to their size and low power requirements. Microrobots at this size scale could be used to add mobility to sensors in large-scale sensor networks as the size of those integrated sensors shrink as shown in [1]. Large numbers of autonomous mobile microrobots could also be used for search in unstructured environments, surveillance, and micro construction tasks.

However, obstacles present a serious challenge to mobility at the millimeter-scale due to the fact that even surface roughness can become an issue for movement. Moving around in an unstructured environment becomes even more difficult. Flying microrobots, such as the one outlined in [2], overcome this predicament by simply ignoring terrestrial considerations. However, such robots can be difficult to control and to design autonomously due to the continuous high power output required from the actuators. Walking microrobots as seen in [3] offer a much simpler design and control problem, but can only overcome obstacles on the same order of magnitude as their leg length.

Efficiency becomes another important issue for mobile robots at the millimeter scale. When the power supply becomes a significant portion of the robot's mass, it is essential to design the robot to move as efficiently as possible. Efficiency can be improved by choosing an appropriate gait and reducing the energy required to move internal pieces of the robot which don't contribute to external motion.

In nature, millimeter-sized insects often address both obstacles and efficiency through jumping. While jumping is often seen as an energetically costly escape mechanism, [4] has shown that as insect size shrinks, jumping becomes more advantageous due to the higher takeoff velocities allowed. Because small jumpers are more mechanically efficient than their larger counterparts, they require less muscle tissue to make them more energy efficient as well. As an example of a jumping insect similarly sized to the proposed robot, the froghopper has a mass of approximately 12 mg and averages 43 cm vertical per jump with a 58^{o} takeoff angle [5].

For the microrobot to gain these same advantages, a jumping gait is proposed. In this paper, jumping is defined as ballistic jumping much like a frog or flea. Continuous jumping, or hopping, requires significant control challenges that are not addressed in the current work. Jumping robots have been demonstrated previously at larger sizes. In [6], a 1.3 kg jumping robot was designed as a potential platform for planetary exploration. Jumps of up to 3 m horizontally and 1.2 m vertically were demonstrated with a single actuator to compress a spring and right itself after a jump. A prototype 10 g robot was designed and simulated in [7] to explore jumping as an option for locomotion at centimeter size scales.

This paper presents the design, fabrication, and some initial results for an autonomous jumping microrobot. Section II will discuss the challenges for jumping at this scale as well as requirements for energy storage, actuation, power, and control. Section III details the fabrication process used to build this microrobot and Section IV discusses some initial results from prototypes.

II. Microrobot Design

The ultimate goal of this project is to create an autonomous mobile microrobot that can move around in unstructured environments. Ideally, this microrobot will be millimeter-sized and be able to jump many centimeters several times per minute. To examine the initial kinetic energies required to produce such jumps, a simple model describing the robot as a point mass of 10 mg (similar mass to [3]) is used to plot various trajectories in Figure 1. Given a specified kinetic energy at the jump take-off, height and distance may be calculated as follows.

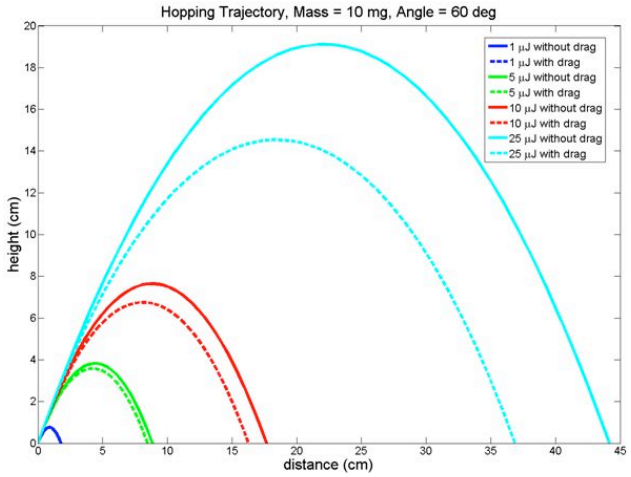

Figure 1. Jumping trajectories given kinetic energy available at take-off.

$$d = 2U_{kinetic} \sin 2\alpha / mg \quad (1)$$

$$h = U_{kinetic} (\sin \alpha)^2 / mg \quad (2)$$

In (1), d is horizontal distance traveled, $U_{kinetic}$ is the kinetic energy available at take-off, α is take-off angle, h is maximum height, m is robot mass, and g is gravity. As can be seen in Figure 1, kinetic energies as small as 1 μJ will still lead to 1.8 cm of horizontal travel over millimeter-sized obstacles and energies of 25 μJ will lead to jumps greater than 40 cm overcoming obstacles over 10 cm high.

However, the height and distance numbers given by (1, 2) are not entirely accurate due to drag effects which are illustrated by the corresponding dashed lines in Figure 1. As the robot size becomes smaller, the frontal area to mass ratio increases which influences the drag forces experienced by the jumping microrobot in flight. Force due to drag is defined by,

$$F_{drag} = C_{drag} \cdot A \cdot \rho \cdot U_{kinetic} / m \quad (3)$$

where C_{drag} is the drag coefficient, A is the frontal area, and ρ is the air density. As can be seen from this equation, the force due to drag increases as the ratio A/m increases, but is also proportional to the initial kinetic energy. Lower initial energies reduce the jumping performance, but also reduce the drag effect calculated in Table 1. An efficiency of 88% with an initial kinetic energy of 10 μJ still provides excellent performance. A thorough study of the effect of drag forces on insects was described in [8], and a conservative estimate of 1.5 for C_{drag} was taken from this reference.

From the numbers shown above and the initial goal of traveling many centimeters per jump, the design of this jumping microrobot aims to provide 10 μJ of kinetic energy at take-off. To accomplish this task, the robot design has been divided into four primary challenges: energy storage, actuation, power, and control. Due to the size scale of this robot and the desire to minimize mass as much as possible, none of these items are readily available off-the-shelf and each will need to be designed and fabricated separately.

Table 1. Drag effects for a jumping microrobot in air.

Energy (μJ)	Velocity (m/s)	Height in vacuum (cm)	Height in air (cm)	Efficiency
1	0.45	0.76	0.75	0.99
5	1.0	3.8	3.6	0.94
10	1.4	7.6	6.8	0.88
25	2.2	19	15	0.76

Mass = 10 mg, $A*C_{drag}$ = 30 mm^2, Angle = 60°

Towards that end, this section discusses the requirements of each subsystem as well as proposed solutions.

A. *Energy Storage*

It was recognized very early that small insects required some sort of energy storage device to jump [9]. As leg length shrinks, so does the time that the robot has to accelerate to its take-off velocity. For millimeter-scale leg lengths, this translates to acceleration times of milliseconds given take-off velocities on the order of 1 m/s as shown in Table 1.

$$t_{acc} = 2l_{leg} / v_{take-off} \quad (4)$$

Assuming a leg length l_{leg} of 5 mm and a take-off velocity $v_{take-off}$ of 1.4 m/s, the actuator acceleration time t_{acc} is 7.1 ms. Since fabricating actuators capable these specifications is quite difficult at this scale, energy storage with quick release provides a much simpler solution.

While insects store energy by compressing resilin pads, a jumping robot can achieve similar results by storing energy in a spring. Given an ideal linear spring, strain energy stored in that spring may be calculated as follows.

$$U_{strain} = 0.5Fx = 0.5kx^2 = 0.5F^2 / k \quad (5)$$

F is the force applied to the spring, x is the distance that the spring is stretched, and k is the spring constant. The forces and distances required to store the energies discussed previously are shown in Figure 2.

Assuming a relatively modest 40% conversion rate from energy stored in the spring to energy available at take-off, a Force/Distance value of 10 mN/5 mm from the 25 μJ curve should be sufficient to provide 10 μJ for the jump. While

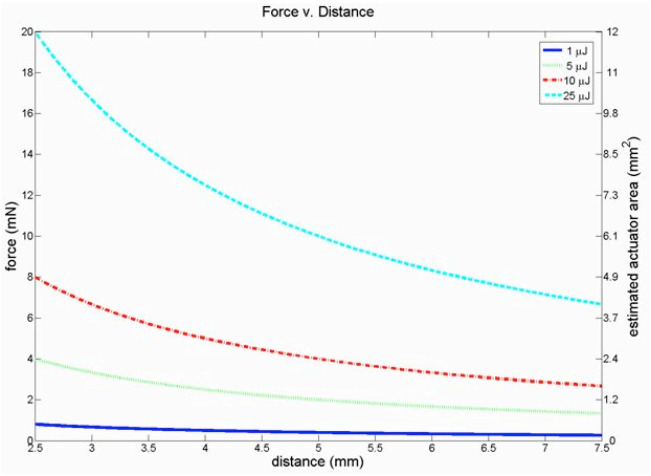

Figure 2. Force v. Distance for various spring storage energies.

any value along this curve may be chosen, these two numbers are chosen as a starting point and design trade-offs may be made later in the design process.

Several other requirements should be taken into consideration when designing the energy storage system for the jumping microrobot. Besides being able to store 25 μJ of energy at moderate forces and displacements, the spring should also have a low mass, simple process integration and a low internal viscosity to minimize energy loss. While silicon is a simple material to use in fabrication at this size scale, it does not match the force/displacement characteristics required due to its low maximum strain of less than 1%. Previous energy storage systems have used polysilicon springs by bending them, but this method inherently stores less energy per volume than putting the spring in tension where the strain is constant throughout the width of the spring [10].

Instead, elastomer materials such as silicone and latex are proposed due to the high strains of several 100% that they can achieve. Examining the mechanical properties alone, silicone compares very favorably to the biological material resilin (Table 2). The maximum energy stored for a beam of area A and length l is proportional both to the material strength (τ) as well as its maximum strain (ε_{max}) of the material.

$$U_{\max} = 0.5Al\tau\varepsilon_{\max} = 0.5AlE\varepsilon_{\max}^2 = 0.5Al\tau^2 / E \qquad (6)$$

Elastomers not only store more energy per volume than silicon, but the material characteristics are more amenable to the forces and distances described above. For example, a silicone beam designed to withstand a 10 mN force and 5 mm displacement would have a length of 1.4 mm and a cross-sectional area of 2900 μm^2. A silicon beam stretched in the same manner would have a length of 1 m and an area of 12.5 μm^2 due to silicon's low maximum strain and high strength.

B. Actuation

Assuming that elastomers have been chosen for the energy storage system, an actuator must now be chosen to store the energy. This actuator requires a long throw of 5 mm, a high force of 10 mN, low power operation, good efficiency, voltage/current compatibility with available power supplies, low mass, and simple fabrication and integration. Electrostatic inchworm motors are a good fit for these requirements and have been demonstrated with energy efficiencies of just under 10% while operating at 33 V [11].

Electrostatic inchworm motors are made up of multiple sets of gap closing actuator arrays (GCAs); two drive arrays which move the shuttle forward and two clutch arrays which connect the drive actuators to the shuttle. Each gap closing actuator is composed of two parallel beams, one of which is fixed to the substrate and the other which is connected through a spring. While a single GCA may only be able to move the length of the gap between the two beams, inchworm motors accumulate these gaps into large travels as seen in Figure 3. This easily satisfies the long throw requirement to store energy in the elastomer spring.

Table 2. Properties of spring materials [12-14].

Material	E (Pa)	Maximum Strain (%)	Tensile Strength (Pa)	Energy Density (mJ/mm^3)
Silicon	169x10^9	0.6	1x10^9	3
Silicone	750x10^3	350	2.6x10^6	4.5
Resilin	2x10^6	190	4x10^6	4

The force available from an inchworm motor comes from the drive actuators. The static force provided by the gap closing actuator arrays can be described as

$$F_{gca} = 0.5N\varepsilon_0 V^2 A / g_0^2 \qquad (7)$$

where N is the number of actuators in the array, ε_0 is the dielectric constant of the air between the beams, A is the actuation area of each beam, g_0 is the initial gap between the beams, and V is the voltage applied between them. At a voltage of 50 V, a 110 element array with initial gaps of 3 μm and area of 50 x 150 μm^2, the actuator force would be 1 mN.

However, new approaches to motor design will allow these force numbers to be pushed even higher and closer to the 10 mN required. Initial gap sizes can be made smaller than allowed by lithographic limits by using a transmission system as seen in Figure 4. The transmission consists of a separate actuator in series with the drive actuator which prevents the drive actuator's restoring springs from pulling it back to the fabricated gap width. In addition, the final gap can be reduced by using integrated nitride gap stops as

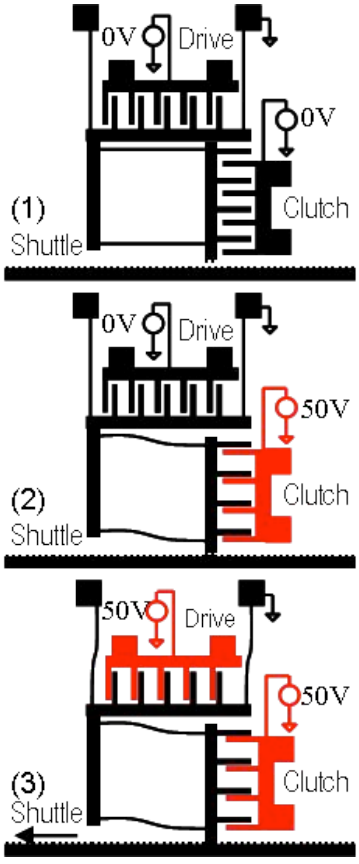

Figure 3. Operation of one half of an electrostatic inchworm motor.

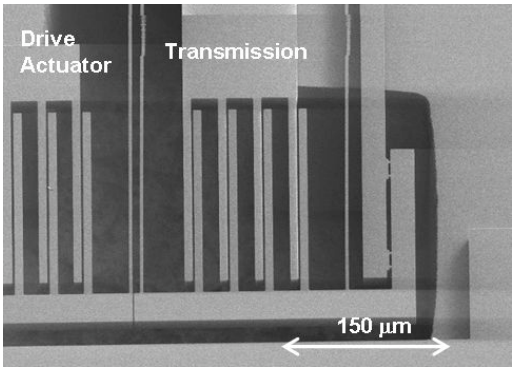

Figure 4. Transmission to reduce initial gap in drive actuator of inchworm motor. Transmission is currently engaged.

shown in [15]. Using integrated nitride gap stops allows larger step sizes and longer beams. At the same voltage of 50 V, a 135 element array with initial gaps of 1.5 μm and an area of 50 x 300 μm^2, the actuator force is now 10 mN.

C. Power

Designing an appropriate power supply for an autonomous jumping microrobot offers one of the most difficult challenges. This power supply should provide enough energy for multiple jumps (preferably rechargeable in some fashion), occupy small area and mass, and offer simple integration to the actuators. As shown above, force provided by the inchworm motor is proportional to E_{max}^2, so it is advantageous to provide a power supply with as high a voltage as possible. Unfortunately, even though they may demonstrate high energy density, most commercial batteries provide voltages on the order of a couple Volts. In order to make these batteries appropriate for use with inchworm motors, additional power circuitry would be required to boost the voltage which requires significant extra area and mass.

Instead, this robot will use the solar cells demonstrated with the microrobot in [3]. By using a silicon-on-insulator (SOI) wafer and trench isolation to separate solar cells, they may be connected in series to achieve higher voltages. In [16], arrays greater than 88 V were demonstrated with efficiencies of up to 14%. Each solar cell chip also provides eight high voltage buffers to amplify signals from the microcontroller to the voltages required to drive the motor. While multiple solar cell array chips are available, the 50 V solar cell arrays to be used on the microrobot are 3.6 x 1.8 mm^2 in area and 2.3 mg and are shown in Figure 5.

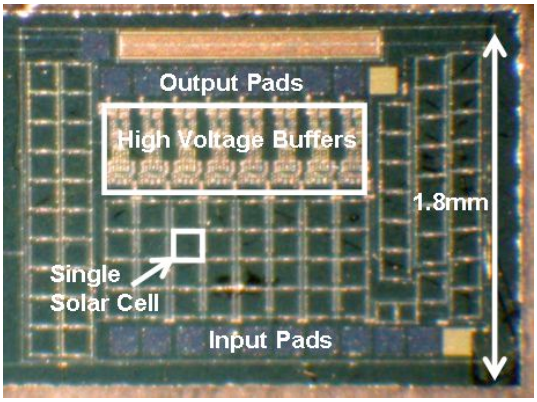

Figure 5. Solar cell chip designed for 50 V signals to motors. Each square is a solar cell connected in series to provide the 50 V required.

D. Control

Finally, the robot requires a controller to sequence the motors at the appropriate times. This controller should be low current due to limited current supplied by the solar cells, small, and simple to integrate. Ideally the controller is also programmable and available off-the-shelf.

EM Microelectronic supplies 4-bit microcontrollers that require no external components and run on 5.8 μA active and 3.3 μA standby current at 2 V [17]. The EM6580 microcontroller has flash memory for reprogrammability as well as 5 output channels which are more than enough to drive a single inchworm motor. These microcontrollers are also small in size at 2 x 2.7 mm^2 and 3.5 mg with the potential of weighing even less if thinned down.

III. Fabrication

In order to keep fabrication as simple as possible, two separate processes are used and the results, along with the solar cells and microcontroller are assembled together. To fabricate elastomer springs for the energy storage system, micro rubber bands are made using a silicon mold. The actuators and robot body are built in a two-mask SOI process. Finally, the results are assembled together.

A. Elastomer Molding

The goal of the elastomer process is to produce high quality springs with good yield which can be easily assembled into silicon microstructures. Silicon molds are fabricated by patterning and etching a silicon wafer using the Surface Technology Systems (STS) Advanced Silicon Etch. The molds are then passivated using C_4F_8 gas at 600 W for 3 minutes. Sylgard® 186 silicone that has been thinned 10:1 with Dow Corning 200® Fluid (50 cst) is then poured into the mold and placed into a 1 torr vacuum for 30 minutes. Finally, the excess silicone is scraped off with a razor blade and the silicone remaining in the trenches is cured at 100C for 45 minutes. After curing, it is possible to simply remove the rubber with tweezers (Figure 8). Three different thicknesses were fabricated, 20 μm, 30 μm, and 40 μm, and characterization results can be found in [12]. Approximately

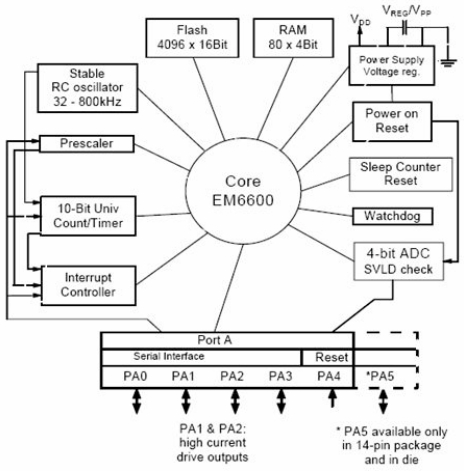

Figure 6. The EM Microelectronic EM6580 architecture [17].

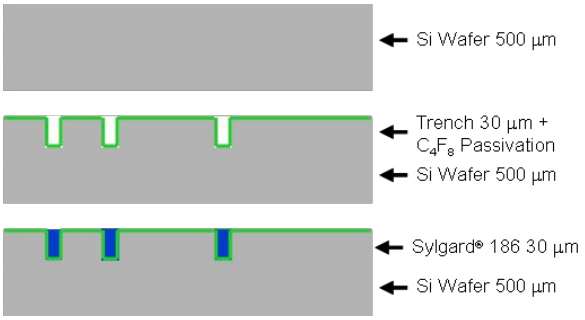

Figure 7. Molding process for fabricating micro rubber bands.

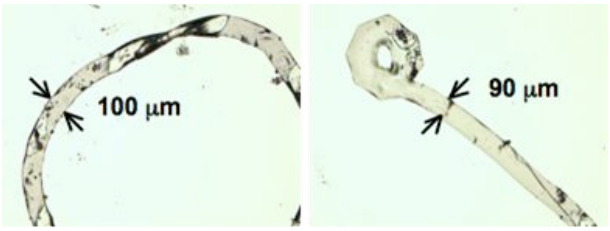

Figure 8. Micro rubber bands of different shapes resulting from molding process.

20 μJ has been stored in these rubber bands by stretching them with a probe tip, which corresponds to a jump height of 20 cm for a 10 mg robot.

B. *Actuators and Robot Body*

The primary goals of the silicon fabrication process are to build actuators capable of storing energy in the micro rubber bands as well as the robot body framework for later assembly. A simple two-mask process that etches both sides of an SOI wafer has been designed (Figure 9). The process starts on a 4-inch SOI wafer with a 20 μm structure layer (frontside), 2 μm buried oxide (BOX), and 300 μm substrate (backside). The front is patterned first and etched using a STS Advanced Silicon Etch. The exposed buried oxide is removed using an RIE oxide etcher and the front is protected by depositing 0.6 μm of low temperature oxide (LTO). The backside is aligned and patterned using a Karl Suss contact printer with backside alignment. Another STS Advanced Silicon Etch is used to etch through the backside, terminating on the BOX layer or LTO deposited earlier. Finally, the structures are released using a timed 49% HF wet etch and a critical point dry.

C. *Assembly*

After both silicon microstructures and micro rubber bands have been fabricated, fine point tweezers are used to assemble rubber bands onto silicon hooks under a stereo inspection microscope (Figure 10). Once the micro rubber band is in place, the silicon may be electrically connected to the other robot components such as the EM6580 microcontroller and solar cells by wirebonding.

IV. Initial Results

Currently, several prototypes have been built to demonstrate system functionality. A small-scale version of the full system has been prototyped with a small solar cell array and the EM6580 driving an inchworm motor. Separately, an inchworm motor has been demonstrated pulling and storing

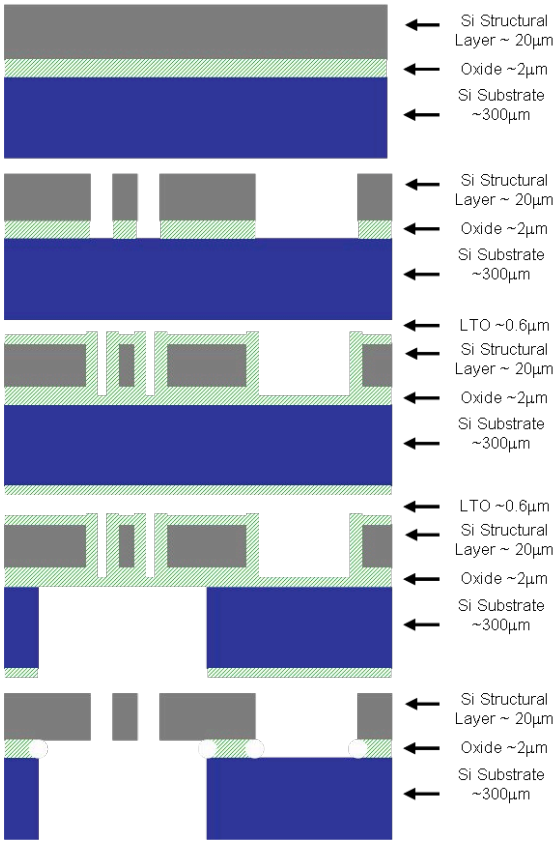

Figure 9. Two mask SOI process for fabricating electrostatic inchworm motors and the rest of the robot body.

energy in a micro rubber band. Finally, a robot prototype has been designed without actuators where the energy is stored by stretching the micro rubber band with a probe tip and releasing the energy quickly.

A. *Solar Cell, Microcontroller, and Inchworm Motor*

For the first prototype system, a small solar cell array has been used to power the EM6580 microcontroller which drives a small inchworm motor. Due to the use of a solar cell array designed to provide approximately 2 μA of current at 1 sun for the microcontroller power, a much higher powered light source was used in testing. The measured open-circuit voltage (Voc) and short-circuit current for the solar cell microcontroller supply were 3.5 V and 15 μA respectively. For the particular solar cell array used, the

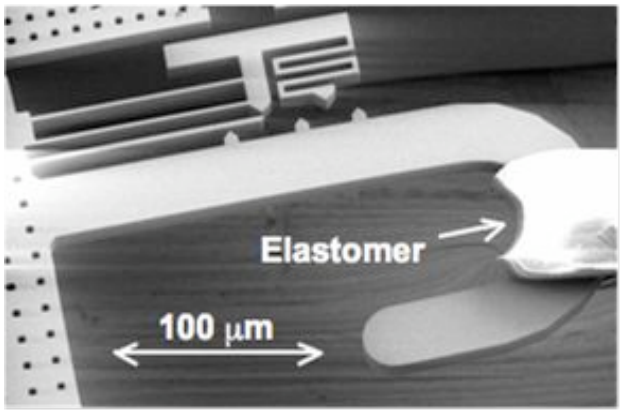

Figure 10. Elastomer assembled onto 20 μm thick silicon hook.

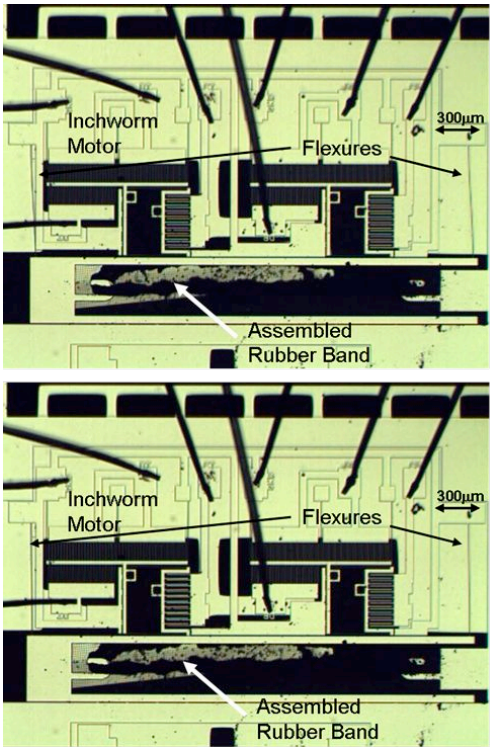

Figure 11. Inchworm motor storing 4.9 nJ in a rubber band and quickly releasing it using the motor clutches.

voltage controlling the inchworm motors was measured at 19 V.

For this test, the solar cell array, microcontroller, and inchworm motor were all bonded into separate packages and wired together on a single breadboard for convenience. Black electrical tape was placed over the high voltage buffers on the solar cell chip to prevent light-related current leakage since a metal light shield was not provided during processing. The microcontroller was programmed to step the inchworm 10 times at a slow speed of 1 Hz for observation. Unfortunately, slipping in the motor's gear teeth prevented the shuttle from moving very far, but it did take 1.5 steps for a total displacement of 6 μm at an estimated force of 2.5 μN. The 50 V solar cells would provide much greater force, but were not used in this test due to limited availability.

B. *Inchworm Motor and Micro Rubber Band*

The second prototype used a separate off-board power supply and controller to store energy in a rubber band using a small inchworm motor (Figure 11). For this test, the inchworm motor was actuated at 90 V for approximately 225 μN of force and displaced 30 μm, at which point the motor's gear teeth began to slip.

To calculate the energy stored by the inchworm motor, it was first necessary to determine the amount of energy stored while assembling the micro rubber band. A load force of 100 μN from pre-straining was estimated by assembling a similarly fabricated micro rubber band into a force gauge elsewhere on the chip. Pre-loading is convenient for assembly, but shifts the force-distance curve above the origin which reduces stored energy for a force-limited motor. For this test, approximately 3 nN was stored due to pre-loading during assembly.

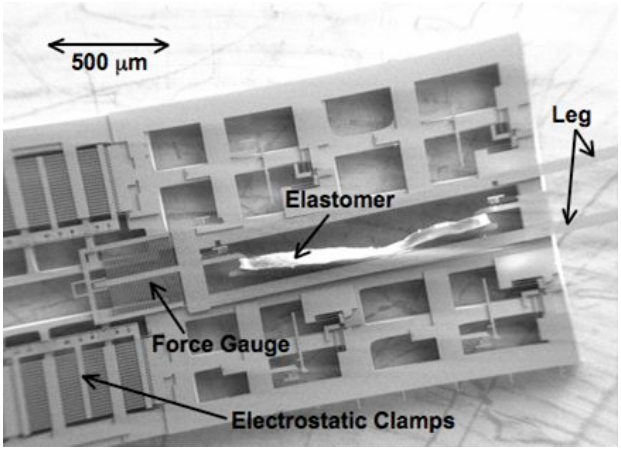

Figure 12. Robot prototype with large electrostatic clamps to hold leg in place before release.

The energy stored by the inchworm motor was calculated by assuming that the maximum force of 225 μN was used towards loading the micro rubber band. Therefore, it was estimated that the inchworm stored an additional 1.9 nN of energy before slipping for a total of 4.9 nN stored and quickly released. Inchworm motors designed more aggressively for larger forces and displacements will push this stored energy significantly higher.

C. *Ballistic Projectiles*

Finally, a prototype robot was built to demonstrate the quick release of energy from a micro rubber band and potentially show an initial jump (Figure 12). This robot consists of a micro rubber band attached to the body of the robot on one side and a leg connected to a force gauge on the other end. In addition, electrostatic GCA clamps are used to hold the leg in place before release. These clamps are designed to be normally-closed so that the clamps open by actuating away from the leg. The advantage of this method over electrostatically closing normally-open clamps is two-fold. Because the flexure force is linear with respect to displacement, the leg self-centers and equal force is provided on both sides of the leg. In addition, the test structure may also be moved and re-oriented while the clamps are held closed.

For testing, the robot was held with double stick tape on a glass slide under a probe station and the leg was pulled back with a probe and clamped to store approximately 1.2 μJ. A 0402-sized capacitor with a mass of approximately 0.6 mg was then maneuvered in front of the leg (Figure 13). Finally, the clamps were actuated to release the leg. While the total energy released is not quantified here, video showed that the leg released its energy in less than a single video frame (66 ms) and the leg propelled the capacitor 1.5 cm along the glass slide. The primary failure mechanism was the leg popping out of plane as seen in the bottom half of Figure 13. In the future, assembled staples over the leg as demonstrated in [18] should be able to fix this problem by preventing the leg from moving vertically out of plane. The 1.2 μJ stored and clamped in this example corresponds to a vertical jump of 1.2 cm for a 10 mg robot. In previous

testing, up to 20 μJ (with a corresponding 20 cm jump) has been stored, but not clamped, in [12].

V. Conclusions and Future Work

This paper presents a design and some initial results towards building an autonomous jumping microrobot. Given the challenge of building this robot at the millimeter scale, the design was broken into four parts, energy storage, actuation, power, and control, and solutions were offered for each. Initial prototypes demonstrate the promise of these solutions.

The next task will involve creating significantly higher force actuators using the transmission design described in Section II and nitride gap stops demonstrated in [15]. These additions will allow the motors to store the microJoules of energy required in the micro rubber bands. Finally, all three components, motors, power, and legs, will be assembled together for autonomous operation. Once the first robots have been successfully assembled, future challenges remain. Robots will need to be designed and fabricated robust enough for multiple jumps. Yet another interesting challenge will be designing for controlled jumps and including sensors on the robot.

Acknowledgments

We would like to thank Seth Hollar and Anita Flynn for fabricating the solar cell arrays used in this paper. We would also like to thank Stratos Christianakis for some initial work in testing the compatibility of the solar cells with the EM6580. Finally, our gratitude goes to the staff and members of the UC Berkeley Microfabrication Laboratory for their advice and assistance.

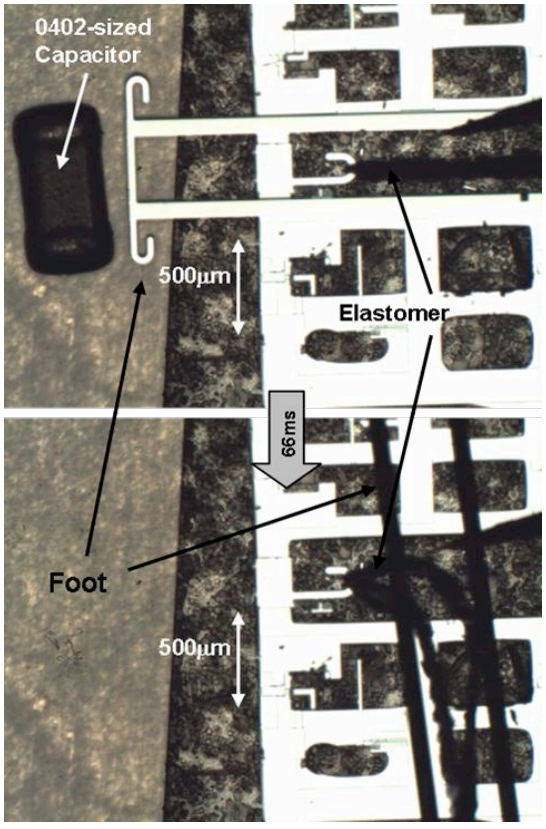

Figure 13. Robot leg propelling an 0402-sized capacitor 1.5 cm along a glass slide. The camera frame rate was 15 fps.

References

[1] B. W. Cook, S. Lanzisera, and K. S. J. Pister, "SoC issues for RF smart dust," *Proceedings of the IEEE,* vol. 94, pp. 1177-1196, June 2006 2006.

[2] J. Yan, R. J. Wood, S. Avadhanula, M. Sitti, and R. S. Fearing, "Towards Flapping Wing Control for a Micromechanical Flying Insect," in *IEEE International Conference on Robotics and Automation*, Seoul, Korea, 2001, pp. 3901-3908.

[3] S. Hollar, A. Flynn, C. Bellew, and K. S. J. Pister, "Solar powered 10 mg silicon robot," in *IEEE Conference on Micro Electro Mechanical Systems*, Kyoto, Japan, 2003, pp. 706-711.

[4] M. N. Scholz, M. F. Bobbert, and A. J. K. v. Soest, "Scaling and jumping: Gravity loses grip on small jumpers," *Journal of Theoretical Biology,* vol. 240, pp. 554-561, June 21 2006 2006.

[5] M. Burrows, "Froghopper insects leap to new heights," *Nature,* vol. 424, p. 509, 31 July 2003 2003.

[6] P. Fiorini and J. Burdick, "The Development of Hopping Capabilities for Small Robots," *Autonomous Robots,* vol. 14, pp. 239-254, 2003.

[7] U. Scarfogliero, C. Stefanini, and P. Dario, "A Bioinspired Concept for High Efficiency Locomotion in Micro Robots: the Jumping Robot Grillo," in *IEEE International Conference on Robotics and Automation*, 2006, pp. 4037-4042.

[8] H. C. Bennet-Clark and G. M. Alder, "The effect of air resistance on the jumping performance of insects," *The Journal of Experimental Biology,* vol. 82, pp. 105-121, 1979.

[9] H. C. Bennet-Clark and E. C. A. Lucey, "The jump of the flea: a study of the energetics and a model of the mechanism," *Journal of Experimental Biology,* vol. 47, pp. 59-76, 1967.

[10] M. S. Rodgers, J. J. Allen, K. D. Meeks, B. D. Jensen, and S. L. Miller, "A microelectromechanical high-density energy storage/rapid release system," in *SPIE*, 1999, pp. 212-22.

[11] R. Yeh, S. Hollar, and K. S. J. Pister, "Single mask, large force, and large displacement electrostatic linear inchworm motors," *Journal of Microelectromechanical Systems,* vol. 11, pp. 330-336, August 2002 2002.

[12] S. Bergbreiter and K. S. J. Pister, "Elastomer-based micromechanical energy storage system," in *ASME International Mechanical Engineering Congress and Exposition*, Chicago, IL, 2006.

[13] J. Gosline, M. Lillie, E. Carrington, P. Guerette, C. Ortlepp, and K. Savage, "Elastic Proteins: biological roles and mechanical properties," *Philosophical Transactions of the Royal Society of London B Biological Sciences,* vol. 357, pp. 121-132, February 28, 2002 2002.

[14] T. Yi and C. J. Kim, "Microscale material testing: etchant effect on the tensile strength," in *International Conference on Solid-State Sensors and Actuators*, Sendai, Japan, 1999, pp. 512-521.

[15] E. Sarajlic, E. Berenschot, G. Krijnen, and M. Elwenspoek, "Versatile trench isolation technology for the fabrication of microactuators," *Microelectronic Engineering,* vol. 67-68, pp. 430-437, 2003.

[16] C. Bellew, S. Hollar, and K. S. J. Pister, "An SOI process for fabrication of solar cells, transistors and electrostatic actuators," in *Transducers*, Boston, MA, 2003, pp. 1075-1078.

[17] E. Microelectronic, "Ultra Low Power 8-pin Flash Microcontroller," in http://www.emmicroelectronic.com/webfiles/product/mcu/ds/EM6580_DS.pdf, 2005.

[18] V. Subramaniam, M. E. Last, and K. S. J. Pister, "Methods and Characterization of Pick and Place Microassembly," in *ASME International Mechanical Engineering Congress and Exposition*, Chicago, IL, 2006.